

Functional imaging of the musculoskeletal system

James F. Griffith

Department of Imaging and Interventional Radiology, The Chinese University of Hong Kong, Prince of Wales Hospital, Shatin, Hong Kong SAR, China

Correspondence to: Prof. James F. Griffith, Department of Imaging and Interventional Radiology, The Chinese University of Hong Kong, Prince of Wales Hospital, Shatin, New Territories, Hong Kong SAR, China. Email: griffith@cuhk.edu.hk.

Abstract: Functional imaging, which provides information of how tissues function rather than structural information, is well established in neuro- and cardiac imaging. Many musculoskeletal structures, such as ligaments, fascia and mineralized bone, have by definition a mainly structural role and clearly don't have the same functional capacity as the brain, heart, liver or kidney. The main functionally responsive musculoskeletal tissues are the bone marrow, muscle and nerve and, as such, magnetic resonance (MR) functional imaging has primarily addressed these areas. Proton or phosphorus spectroscopy, other fat quantification techniques, perfusion imaging, BOLD imaging, diffusion and diffusion tensor imaging (DTI) are the main functional techniques applied. The application of these techniques in the musculoskeletal system has mainly been research orientated where they have already greatly enhanced our understanding of marrow physiology, muscle physiology and neural function. Going forwards, they will have a greater clinical impact helping to bridge the disconnect often seen between structural appearances and clinical symptoms, allowing a greater understanding of disease processes and earlier recognition of disease, improving prognostic prediction and optimizing the monitoring of treatment effect.

Keywords: Functional; imaging; magnetic resonance (MR); perfusion; spectroscopy; BOLD; diffusion; diffusion tensor imaging (DTI)

Submitted Feb 27, 2015. Accepted for publication Feb 28, 2015.

doi: 10.3978/j.issn.2223-4292.2015.03.07

View this article at: <http://dx.doi.org/10.3978/j.issn.2223-4292.2015.03.07>

Functional imaging has been a buzz word for the last 5-10 years. It has been widely adopted in neuroimaging and, also to a lesser extent, cardiac imaging. Particularly with regard to neuroimaging, functional imaging has bridged the gap between experimental research and clinical imaging.

What is functional imaging? Musculoskeletal imaging is for the most part about achieving higher and higher resolution morphological imaging (*Figure 1*). Functional imaging provides information on the physiologic properties rather than the structural properties of the musculoskeletal system. This is the essence of functional imaging.

How does this differ from other types of non-conventional imaging? There is, as expected, an overlap between functional imaging with other types of non-conventional imaging such as molecular imaging, biomechanical imaging, kinetic imaging and other specialized tissue interrogation

techniques. Molecular imaging addresses the characterization and measurement of biological processes at a molecular and cellular level and is generally the prerogative of PET or SPECT imaging. Biomedical imaging usually relates to the microarchitectural composition and relative strength of living tissues with detailed computational analysis as well as finite element modeling and virtual stress testing. Kinetic imaging is used to assess tissue movement while other tissue interrogation techniques such as ultrasound or MR elastography, T1 rho imaging or delayed gadolinium-enhanced magnetic resonance imaging (MRI) of cartilage (dGEMRIC) provide additional information about specific tissues.

Not all tissues in the musculoskeletal system are as receptive to functional imaging as other tissues. For example, some tissues are relatively inert (such as ligaments, tendons



Figure 1 High resolution proton density image of the wrist. Note the clear visibility of the intermediate intensity hyaline articular cartilage (arrow) and the hypointense fibrocartilage of the articular disc (open arrow).

or menisci) and serve a primary structural or locomotive role with relatively little in the way of demonstrable physiological activity. Other tissues such as the bone marrow, the synovium, skeletal muscle and the spinal cord are more physiologically active and more receptive to functional imaging. The main types of functional imaging used in MSK imaging are MR perfusion, MR spectroscopy, diffusion-weighted imaging, diffusion tensor imaging (DTI) and BOLD imaging. Each of these will be discussed in turn.

Perfusion imaging is assessed using dynamic contrast-enhanced MRI. This involves the rapid acquisition of serial MR images during and after administration of MR contrast agent. Based on the time following injection and the concentration of contrast in the tissues under investigation, a time intensity curve can be drawn allowing detection and quantification of ‘wash-in’ and ‘wash-out’ contrast kinetics. Perfusion imaging measures tissue perfusion which is different to tissue blood flow. While blood flow refers to flow within vessels, perfusion is much more encompassing and physiologically relevant parameter that incorporates blood flow, though also capillary permeability and interstitial diffusion. Various quantitative parameters can be used to classify the time intensity curve. The most robust of these parameters are the enhancement slope and enhancement maximum. Enhancement slope refers to the incline of the upright sweep of the time intensity curve

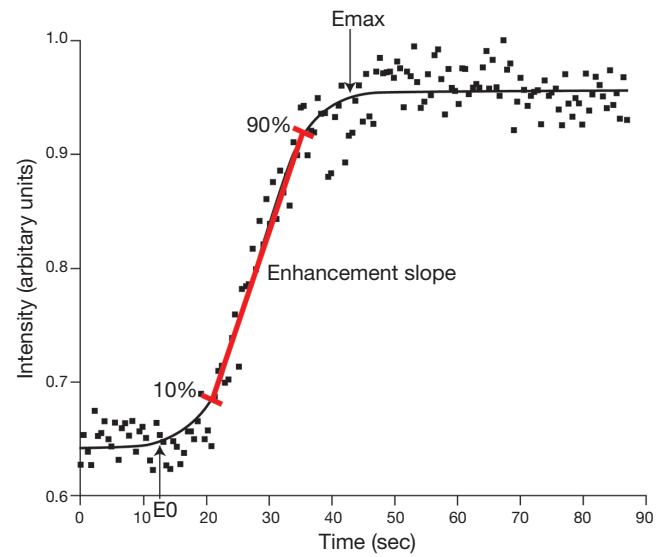


Figure 2 Time-intensity curve of dynamic contrast enhanced MRI following curve fitting of data points. The line representing E_{slope} and the E_{max} point are shown. MRI, magnetic resonance imaging.

usually taken between 10-90% of the length of the upward sweep. E_{max} is the maximum intensity achieved (Figure 2). Pharmacokinetic models have also been applied to the time intensity curve though do tend to be limited in clinical practice by great variability in measurements, particularly arterial input function (AIF) though also transfer constant (K_{trans}) and efflux rate constant (k_{ep}) which are strongly influenced by noise and AIF variation (1,2). The parameters, extravascular extracellular space (V_e) or amplitude (A) are more robust and preferable. To help overcome these difficulties, it may be possible to use an internal reference tissue such as skeletal muscle as a comparative standard. That said some studies have shown good reliability of pharmacokinetic perfusion parameters (3).

MR perfusion techniques can be used to assess the perfusion of any tissue within the area of interest, either bone or soft tissue. In practice, the two main areas where perfusion imaging is clinically applicable at the moment are in the assessment of scaphoid perfusion and also in the assessment of synovial activity. Physiologically, all the carpal bones seem to have a comparable level of perfusion (4). For fractures of the waist of the scaphoid, because the blood flow to the scaphoid bone is retrograde though the distal pole, proximal pole perfusion can be compromised. This is not an all or none phenomenon and various degrees of proximal pole ischaemia can exist. Although, one would

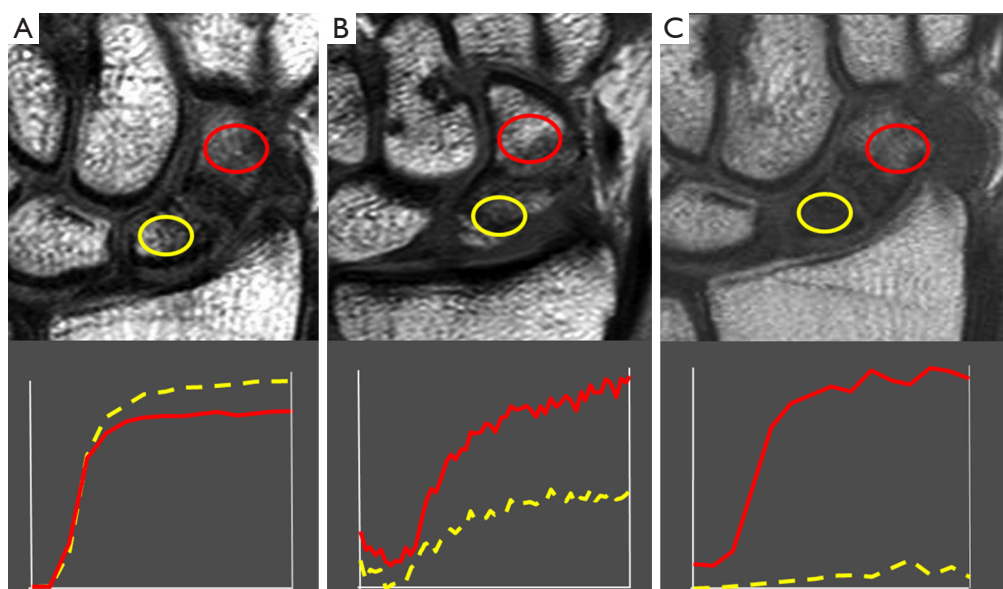


Figure 3 (A-C) Time intensity perfusion curves of three different patients with fractures of the waist of scaphoid. The proximal pole of the right hand image (A) has good perfusion while of the left hand image (C) has no perfusion i.e., is avascular. The proximal pole of the middle image (B) is poorly perfused (i.e., is ischaemic) as the E_{max} and E_{slope} are less the 50% those present in the distal pole.

inherently think that perfusion imaging would be helpful in the assessment of scaphoid vascularity, this has not been a consistent finding with some studies advocating (5,6) and others less enthusiastic (7,8) about the technique.

Similar studies have been performed on the proximal femur where the femoral head is prone to avascular necrosis following fractures of the femoral head. The femoral head is inherently very poorly perfused compared to other skeletal areas (9). In osteoporosis, perfusion throughout the proximal femur is even further decreased especially in the femoral neck region (10). Femoral neck fractures have a high incidence of avascular necrosis and non-union (11). Perfusion imaging is useful for addressing the effect of different surgical dislocation techniques on femoral head perfusion (12), compromised femoral head perfusion following femoral neck fracture (13) and predicting non-union or avascular necrosis (14,15). An E_{max} or E_{slope} on the fractured side of <30% that of the contralateral non-fractured side seems a good indicator of subsequent avascular necrosis and non-union (14,15) (*Figure 3*).

Perfusion imaging can also be used to assess synovial activity. Synovial activity can be assessed by measuring the degree (volume) of synovial proliferation and its perfusion. In patients commencing anti-biologic agent such as TNF alpha blocker, a reduction in synovial perfusion seems to be a more sensitive indicator of response than synovial volume (16,17)

(*Figure 4*). Dynamic contrast enhanced MRI may also be useful in the detection of early rheumatoid arthritis (18).

PET imaging can also be used to assess bone perfusion using ^{18}F -fluoride ion which has a half-life of 112 minutes. Complete extraction of ^{18}F -fluoride as it passes through bone in the first few minutes following injection allows for assessment of bone blood perfusion using dynamic PET time-activity curves while uptake after 45 min reflects bone turnover (19). Pure bone perfusion can be evaluated by PET using the freely diffusible tracer ^{15}O which has a half-life of only two minutes and requires an on-site cyclotron. Highly significant correlation between blood perfusion measured using ^{18}F -fluoride and true bone perfusion using oxygen-15 has been shown in porcine bone (20). PET can provide bone metabolism data as well as bone blood perfusion data, is not limited by respiration and field of view, and can be used in subjects with renal failure. The main disadvantages are that it needs access to a PET-CT imaging system, does involve ionizing radiation and is more costly than MR and generally more time consuming (each examination can take up to 2 hours).

Following treatment of Paget's disease with bisphosphonates, kinetic parameters, including plasma clearance of fluoride, reduced by about 25% after one month and a further 25% by about 6 months in nearly all patients. Dynamic PET imaging was more perceptible to

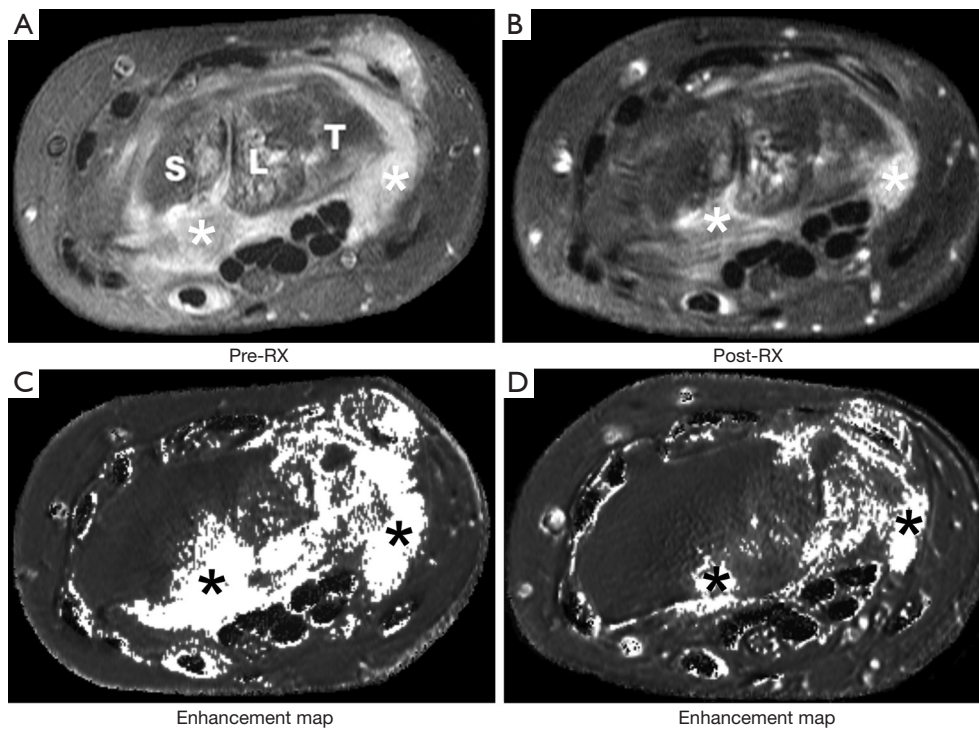


Figure 4 (A,B) Axial MRI images of the wrist showing enhancement maps of synovium pre- and post-treatment (Rx). The enhancement map represents all of those pixels which enhance to a greater degree than muscle tissue (using thenar or hypothenar muscle as a reference standard) and is indicative of enhancing synovium (*). The volume of enhancing synovium decreases appreciably following treatment. MRI, magnetic resonance imaging.

pagetic change than biochemical markers. A similar effect of reduced perfusion in treated pagetic bone was shown by DCE-MRI with reduction in bone perfusion being greater in bisphosphonate-naïve patients than in those previously treated (21). DCE-MRI may be beneficial in determining disease free survival in osteosarcoma (22), for identifying response to chemotherapy (23), disease free survival and overall survival in acute myeloid leukemia (24,25). An animal-based model study has shown delayed contrast wash-out in the normal femoral head compared to other bone areas, which may have implications for conditions such as steroid-induced osteonecrosis (26). Perfusion bone imaging by MRI in guinea pigs with varying severity of osteoarthritis showed how osteoarthritis was associated with decreased subchondral bone flow though no change in permeability or increased intravascular thrombosis (27,28). A decrease in perfusion in medial tibial subchondral bone was observed at 6 and 9 months and temporally preceded the development of cartilage and bone osteoarthritic changes suggesting venous obstruction as an potential underlying mechanism though no cause and effect was established

(19,28). ^{18}F -fluoride PET has been used to study blood flow in allogenic bone grafting (29), joint replacement (30,31) and fracture healing (19,32). DCE-MRI can also be used to assess diffusion into relatively non-vascular structures such as the intervertebral disc (33) with reduced second wash-in phase of E_{max} and E_{slope} seen in ovariectomised rats (Figure 5). This may help explain why post-menopausal women have accelerated disc degeneration (34).

MR spectroscopy (MRS) uses the same basic principles as standard MRI. However, instead of generating an image, the chemical shift of the permitted signal is detected. MRS yields quantitative information on the chemicals that reside within the tissue. The most commonly measured elements in the musculoskeletal system are hydrogen, phosphorus and sodium. Because the MRS is spectrum that is weak, a large volume, usually around 1 cm^2 , needs to be used compared to standard MRI imaging. The most common type of MRS used in musculoskeletal imaging is proton MRS which measures the fat water ratio to obtain the relative amount of fat within the tissues (Figure 6). This is principally applied to the assessment of the bone marrow were MRS is a quite

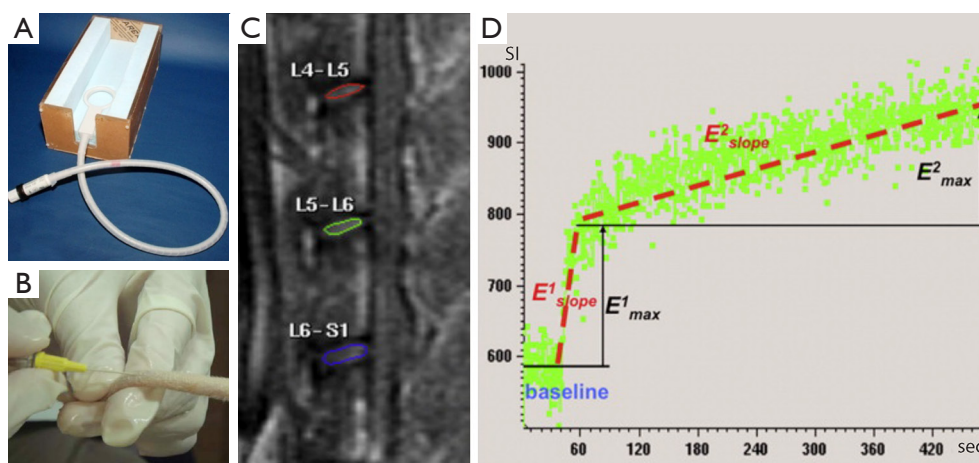


Figure 5 (A-D) Series of images showing set up and results for perfusion imaging of intervertebral disc in a rat. (A) Wooden cradle for holding the anaesthetized rat; (B) cannulation of rat tail vein; (C) regions of interest placed on the intervertebral discs. The normal rat has six lumbar vertebrae.

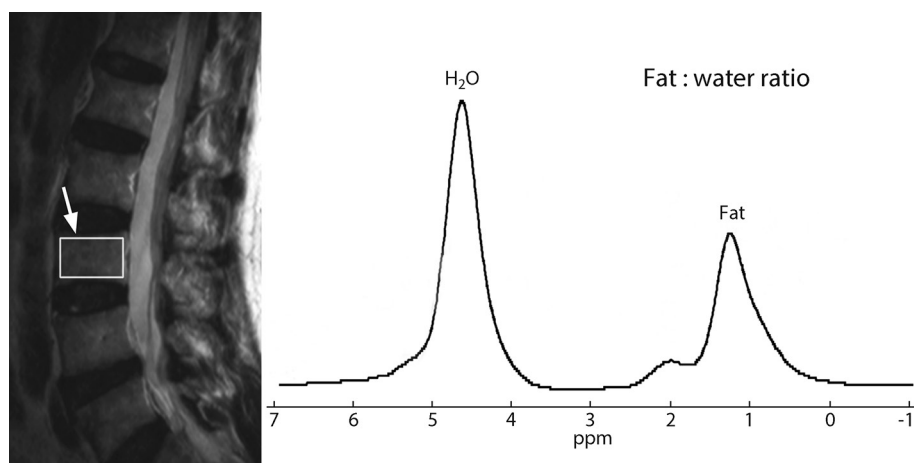


Figure 6 Proton MRS of lumbar vertebral body. MRS assesses the fat peak: water peak ratio. In this example, the marrow is predominantly comprised of red or functioning marrow with a relatively high water peak than fat peak. MRS, magnetic resonance spectroscopy.

highly reached reducible technique (35).

Limitations of MRS are that it assumes a constant amount of water is present within the marrow, only one volume of interest (VOI) can be studied at any given time, and only semi-quantitative information on the amount of fat present is obtained (% fat content rather than g/cm^2). An alternative method of quantifying marrow fat is to use the IDEAL or DIXON method (Figure 7). This IDEAL method uses different pulse sequencing to produce either fat only or water only images. It has advantages over proton MRS in that multiple bone regions can be studied

simultaneously and it tends to be less machine-dependent. The limitation is that you get no indication as to the type of fat present.

Proton MRS has been used to studied bone marrow showing how marrow fat increases throughout life. Marrow fat is about 10-15% more abundant in young males than young females though around the time of the menopause, there is a dramatic increase in marrow fat in female subjects such that after the menopause females contain about 10-15% more fat than male subjects (36). This change in marrow fat composition around the time of the menopause

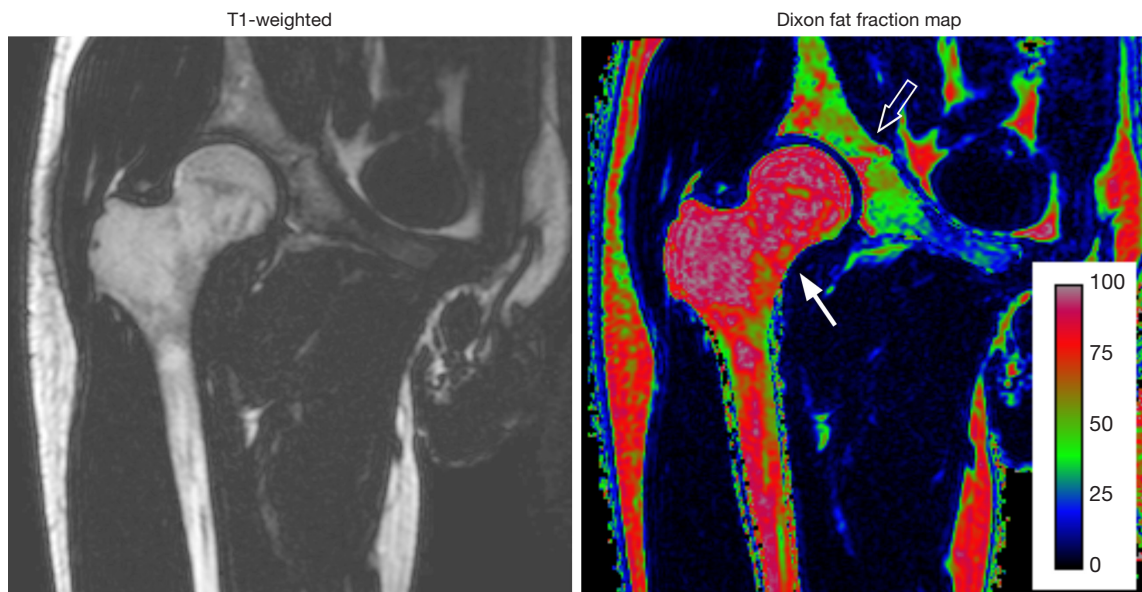


Figure 7 Dixon fat quantification technique provides a measure of relative amount of water or fat on a pixel by pixel basis. When compared to T1-weighted imaging, where fatty marrow is hyperintense and red marrow is isotense to muscle, one can appreciate the predominantly fatty marrow of the proximal femur (arrow) compared to the predominantly red marrow of the acetabulum (open arrow).

corresponds to a decrease in bone mass at that time and may well be related to a shift in mesenchymal stem cell differentiation along adipocytic rather than osteoblastic or haematological cell lines.

There are up to 22 different fatty acids present within the marrow fat with different percentages of saturated and saturated fats (37). MRI study has shown that a decrease in bone mineral density is associated with an increase in marrow fat saturation in osteoporosis as well as in anorexia nervosa (38,39). Interestingly, an increase in marrow fat content was also associated with an increase in intramyocellular lipid content (39). With increasing field strength and coil development, it is likely that a more detailed analysis of the MRS profile will be available in future (40).

Phosphorus MRS has been providing an insight into muscle metabolism for 25 years. The metabolites that can be measured are inorganic phosphate (Pi), phosphocreatine (PCr), and adenosine triphosphate (ATP) while the concentration of adenosine diphosphate (ADP) and the intracellular pH value can be calculated from the biochemistry reaction equilibrium (41). During exercise, the concentration of Pi increases while that of PCr decreases. The Pi/PCr ratio is a measure of oxidative phosphorylation.

In diabetics at rest, the concentration of Pi, PCr and ATP were found to be significantly lower at rest while the

concentration of ADP and Pi/PCr ratio were higher (42). The same increase in Pi and decrease in PCr is seen in diabetic patients as normal subjects though in diabetic patients the recovery rates are slower helping to confirm a skeletal mitochondrial abnormality (42). A mitochondrial disorder is now considered the basis for insulin resistance in tissue so one can see how this change in phosphorylation can be used as a marker of mitochondrial function.

DTI has been used primarily to look at neural disorders using parameters such as apparent diffusion coefficient (ADC) which measures the magnitude of water diffusion within tissues; fractional anisotropy (FA) which describes the degree of anisotropy of this diffusion with eigenvectors (V1, V2 and V3) and their corresponding eigenvalues providing a directional component. "Axial" and "radial" diffusivities are associated with λ_1 and the average of λ_2 and λ_3 respectively. At the carpal tunnel, the FA, radial diffusivity, and ADC differed significantly between healthy subjects and carpal tunnel syndrome patients ($P < 0.0002$) (41,43-45). In healthy subjects, FA increased (+20%, $P < 0.001$) and radial diffusivity and ADC decreased (by -15% and -8%, respectively, $P < 0.05$) when compared the median nerve proximal to the carpal tunnel with that within the carpal tunnel (45). The opposite was seen in CTS subjects where FA decreased (by -21%, $P < 0.05$) and radial diffusivity increased (by +23%, $P < 0.01$) when one compared the median nerve proximal to

the carpal tunnel to that within the carpal tunnel (45).

DTI has also been applied to the study of osteoporosis (46). Mean diffusivity (MD) which is a measure of diffusivity along several directions and FA were able to discriminate either osteoporotic or osteopenic subjects from normal subjects and was better than fat fraction (FF) in this respect. A highly significant positive correlation was found between FA and T-score in all groups together, in healthy and in osteoporotic groups. MD/FF and FA/FF proved more discriminatory than MD and FA alone and in the femoral neck region correctly separated all healthy subjects (46).

In conclusion, one can appreciate that functional imaging in the musculoskeletal system is more than just hype. It can provide useful additional information over and above that available on structural imaging. It is still very much in the experimental stage but similar to functional imaging of say the brain, functional imaging of the musculoskeletal system will move more into the clinical arena for problem solving of selected areas in the not too distant future.

Acknowledgements

This study was partially supported by grants from the Research Grants Council of the Hong Kong SAR (Project No. SEG_CUHK02).

Disclosure: The authors declare no conflict of interest.

References

- Zwick S, Brix G, Tofts PS, Strecker R, Kopp-Schneider A, Laue H, Semmler W, Kiessling F. Simulation-based comparison of two approaches frequently used for dynamic contrast-enhanced MRI. *Eur Radiol* 2010;20:432-42.
- Ma HT, Griffith JF, Yeung DK, Leung PC. Modified brix model analysis of bone perfusion in subjects of varying bone mineral density. *J Magn Reson Imaging* 2010;31:1169-75.
- Breault SR, Heye T, Bashir MR, Dale BM, Merkle EM, Reiner CS, Faridi KF, Gupta RT. Quantitative dynamic contrast-enhanced MRI of pelvic and lumbar bone marrow: effect of age and marrow fat content on pharmacokinetic parameter values. *AJR Am J Roentgenol* 2013;200:W297-303.
- Müller GM, Månsson S, Müller MF, Ekberg O, Björkman A. Assessment of perfusion in normal carpal bones with dynamic gadolinium-enhanced MRI at 3 Tesla. *J Magn Reson Imaging* 2013;38:168-72.
- Ng AW, Griffith JF, Taljanovic MS, Li A, Tse WL, Ho PC. Is dynamic contrast-enhanced MRI useful for assessing proximal fragment vascularity in scaphoid fracture delayed and non-union? *Skeletal Radiol* 2013;42:983-92.
- Schoierer O, Bloess K, Bender D, Burkholder I, Kauczor HU, Schmidmaier G, Weber MA. Dynamic contrast-enhanced magnetic resonance imaging can assess vascularity within fracture non-unions and predicts good outcome. *Eur Radiol* 2014;24:449-59.
- Donati OF, Zanetti M, Nagy L, Bode B, Schweizer A, Pfirrmann CW. Is dynamic gadolinium enhancement needed in MR imaging for the preoperative assessment of scaphoidal viability in patients with scaphoid nonunion? *Radiology* 2011;260:808-16.
- Larribe M, Gay A, Freire V, Bouvier C, Chagnaud C, Souteyrand P. Usefulness of dynamic contrast-enhanced MRI in the evaluation of the viability of acute scaphoid fracture. *Skeletal Radiol* 2014;43:1697-703.
- Griffith JF, Yeung DK, Tsang PH, Choi KC, Kwok TC, Ahuja AT, Leung KS, Leung PC. Compromised bone marrow perfusion in osteoporosis. *J Bone Miner Res* 2008;23:1068-75.
- Wang YX, Griffith JF, Kwok AW, Leung JC, Yeung DK, Ahuja AT, Leung PC. Reduced bone perfusion in proximal femur of subjects with decreased bone mineral density preferentially affects the femoral neck. *Bone* 2009;45:711-5.
- Kaushik A, Sankaran B, Varghese M. To study the role of dynamic magnetic resonance imaging in assessing the femoral head vascularity in intracapsular femoral neck fractures. *Eur J Radiol* 2010;75:364-75.
- Lazaro LE, Sculco PK, Pardee NC, Klinger CE, Dyke JP, Helfet DL, Su EP, Lorich DG. Assessment of femoral head and head-neck junction perfusion following surgical hip dislocation using gadolinium-enhanced magnetic resonance imaging: a cadaveric study. *J Bone Joint Surg Am* 2013;95:e1821-8.
- Dyke JP, Lazaro LE, Hettrich CM, Hentel KD, Helfet DL, Lorich DG. Regional analysis of femoral head perfusion following displaced fractures of the femoral neck. *J Magn Reson Imaging* 2015;41:550-4.
- Kaushik A, Sankaran B, Varghese M. To study the role of dynamic magnetic resonance imaging in assessing the femoral head vascularity in intracapsular femoral neck fractures. *Eur J Radiol* 2010;75:364-75.
- Hirata T, Konishiike T, Kawai A, Sato T, Inoue H. Dynamic magnetic resonance imaging of femoral head perfusion in femoral neck fracture. *Clin Orthop Relat Res*

- 2001;(393):294-301.
16. Meier R, Thuermel K, Noël PB, Moog P, Sievert M, Ahari C, Nasirudin RA, Golovko D, Haller B, Ganter C, Wildgruber M, Schaeffeler C, Waldt S, Rummeny EJ. Synovitis in patients with early inflammatory arthritis monitored with quantitative analysis of dynamic contrast-enhanced optical imaging and MR imaging. *Radiology* 2014;270:176-85.
 17. Tam LS, Griffith JF, Yu AB, Li TK, Li EK. Rapid improvement in rheumatoid arthritis patients on combination of methotrexate and infliximab: clinical and magnetic resonance imaging evaluation. *Clin Rheumatol* 2007;26:941-6.
 18. Axelsen MB, Ejbjerg BJ, Hetland ML, Skjødt H, Majgaard O, Lauridsen UB, Hørslev-Petersen K, Boesen M, Kubassova O, Bliddal H, Østergaard M. Differentiation between early rheumatoid arthritis patients and healthy persons by conventional and dynamic contrast-enhanced magnetic resonance imaging. *Scand J Rheumatol* 2014;43:109-18.
 19. Dyke JP, Aaron RK. Noninvasive methods of measuring bone blood perfusion. *Ann N Y Acad Sci* 2010;1192:95-102.
 20. Piert M, Machulla HJ, Jahn M, Stahlschmidt A, Becker GA, Zittel TT. Coupling of porcine bone blood flow and metabolism in high-turnover bone disease measured by [(15)O]H(2)O and [(18)F]fluoride ion positron emission tomography. *Eur J Nucl Med Mol Imaging* 2002;29:907-14.
 21. Libicher M, Kasperk C, Daniels-Wredenhagen M, Heye T, Kauczor HU, Nawroth P, Delorme S, Hosch W. Dynamic contrast-enhanced MRI for monitoring bisphosphonate therapy in Paget's disease of bone. *Skeletal Radiol* 2013;42:225-30.
 22. Guo J, Reddick WE, Glass JO, Ji Q, Billups CA, Wu J, Hoffer FA, Kaste SC, Jenkins JJ, Ortega Flores XC, Quintana J, Villarroel M, Daw NC. Dynamic contrast-enhanced magnetic resonance imaging as a prognostic factor in predicting event-free and overall survival in pediatric patients with osteosarcoma. *Cancer* 2012;118:3776-85.
 23. Hou HA, Shih TT, Liu CY, Chen BB, Tang JL, Yao M, Huang SY, Chou WC, Hsu CY, Tien HF. Changes in magnetic resonance bone marrow angiogenesis on day 7 after induction chemotherapy can predict outcome of acute myeloid leukemia. *Haematologica* 2010;95:1420-4.
 24. Chen BB, Hsu CY, Yu CW, Hou HA, Liu CY, Wei SY, Chou WC, Tien HF, Shih TT. Dynamic contrast-enhanced MR imaging measurement of vertebral bone marrow perfusion may be indicator of outcome of acute myeloid leukemia patients in remission. *Radiology* 2011;258:821-31.
 25. Shih TT, Hou HA, Liu CY, Chen BB, Tang JL, Chen HY, Wei SY, Yao M, Huang SY, Chou WC, Hsu SC, Tsay W, Yu CW, Hsu CY, Tien HF, Yang PC. Bone marrow angiogenesis magnetic resonance imaging in patients with acute myeloid leukemia: peak enhancement ratio is an independent predictor for overall survival. *Blood* 2009;113:3161-7.
 26. Wang YX, Griffith JF. Menopause causes vertebral endplate degeneration and decrease in nutrient diffusion to the intervertebral discs. *Med Hypotheses* 2011;77:18-20.
 27. Dyke JP, Synan M, Ezell P, Ballon D, Racine J, Aaron RK. Characterization of bone perfusion by dynamic contrast-enhanced magnetic resonance imaging and positron emission tomography in the Dunkin-Hartley guinea pig model of advanced osteoarthritis. *J Orthop Res* 2015;33:366-72.
 28. Aaron RK, Dyke JP, Ciombor DM, Ballon D, Lee J, Jung E, Tung GA. Perfusion abnormalities in subchondral bone associated with marrow edema, osteoarthritis, and avascular necrosis. *Ann N Y Acad Sci* 2007;1117:124-37.
 29. Sörensen J, Ullmark G, Långström B, Nilsson O. Rapid bone and blood flow formation in impacted morselized allografts: positron emission tomography (PET) studies on allografts in 5 femoral component revisions of total hip arthroplasty. *Acta Orthop Scand* 2003;74:633-43.
 30. Piert M, Machulla HJ, Jahn M, Stahlschmidt A, Becker GA, Zittel TT. Coupling of porcine bone blood flow and metabolism in high-turnover bone disease measured by [(15)O]H(2)O and [(18)F]fluoride ion positron emission tomography. *Eur J Nucl Med Mol Imaging* 2002;29:907-14.
 31. Temmerman OP, Raijmakers PG, Heyligers IC, Comans EF, Lubberink M, Teule GJ, Lammertsma AA. Bone metabolism after total hip revision surgery with impacted grafting: evaluation using H2 15O and [18F]fluoride PET; a pilot study. *Mol Imaging Biol* 2008;10:288-93.
 32. Hsu WK, Feeley BT, Krenek L, Stout DB, Chatziioannou AF, Lieberman JR. The use of 18F-fluoride and 18F-FDG PET scans to assess fracture healing in a rat femur model. *Eur J Nucl Med Mol Imaging* 2007;34:1291-301.
 33. Deng M, Griffith JF, Zhu XM, Poon WS, Ahuja AT, Wang YX. Effect of ovariectomy on contrast agent diffusion into lumbar intervertebral disc: a dynamic contrast-enhanced MRI study in female rats. *Magn Reson Imaging* 2012;30:683-8.
 34. Wang YX, Griffith JF. Effect of menopause on lumbar

- disk degeneration: potential etiology. *Radiology* 2010;257:318-20.
35. Griffith JF, Wang YX, Zhou H, Kwong WH, Wong WT, Sun YL, Huang Y, Yeung DK, Qin L, Ahuja AT. Reduced bone perfusion in osteoporosis: likely causes in an ovariectomy rat model. *Radiology* 2010;254:739-46.
 36. Griffith JF, Yeung DK, Ma HT, Leung JC, Kwok TC, Leung PC. Bone marrow fat content in the elderly: a reversal of sex difference seen in younger subjects. *J Magn Reson Imaging* 2012;36:225-30.
 37. Griffith JF, Yeung DK, Chow SK, Leung JC, Leung PC. Reproducibility of MR perfusion and (1)H spectroscopy of bone marrow. *J Magn Reson Imaging* 2009;29:1438-42.
 38. Yeung DK, Griffith JF, Antonio GE, Lee FK, Woo J, Leung PC. Osteoporosis is associated with increased marrow fat content and decreased marrow fat unsaturation: a proton MR spectroscopy study. *J Magn Reson Imaging* 2005;22:279-85.
 39. Bredella MA, Fazeli PK, Daley SM, Miller KK, Rosen CJ, Klibanski A, Torriani M. Marrow fat composition in anorexia nervosa. *Bone* 2014;66:199-204.
 40. Ren J, Dimitrov I, Sherry AD, Malloy CR. Composition of adipose tissue and marrow fat in humans by 1H NMR at 7 Tesla. *J Lipid Res* 2008;49:2055-62.
 41. Bulut HT, Yildirim A, Ekmekci B, Gunbey HP. The diagnostic and grading value of diffusion tensor imaging in patients with carpal tunnel syndrome. *Acad Radiol* 2014;21:767-73.
 42. Wu FY, Tu HJ, Qin B, Chen T, Xu HF, Qi J, Wang DH. Value of dynamic ³¹P magnetic resonance spectroscopy technique in in vivo assessment of the skeletal muscle mitochondrial function in type 2 diabetes. *Chin Med J (Engl)* 2012;125:281-6.
 43. Lindberg PG, Feydy A, Le Viet D, Maier MA, Drapé JL. Diffusion tensor imaging of the median nerve in recurrent carpal tunnel syndrome - initial experience. *Eur Radiol* 2013;23:3115-23.
 44. Naraghi A, da Gama Lobo L, Menezes R, Khanna M, Sussman M, Anastakis D, White LM. Diffusion tensor imaging of the median nerve before and after carpal tunnel release in patients with carpal tunnel syndrome: feasibility study. *Skeletal Radiol* 2013;42:1403-12.
 45. Stein D, Neufeld A, Pasternak O, Graif M, Patish H, Schwimmer E, Ziv E, Assaf Y. Diffusion tensor imaging of the median nerve in healthy and carpal tunnel syndrome subjects. *J Magn Reson Imaging* 2009;29:657-62.
 46. Manenti G, Capuani S, Fanucci E, Assako EP, Masala S, Sorge R, Iundusi R, Tarantino U, Simonetti G. Diffusion tensor imaging and magnetic resonance spectroscopy assessment of cancellous bone quality in femoral neck of healthy, osteopenic and osteoporotic subjects at 3T: Preliminary experience. *Bone* 2013;55:7-15.

Cite this article as: Griffith JF. Functional imaging of the musculoskeletal system. *Quant Imaging Med Surg* 2015;5(3):323-331. doi: 10.3978/j.issn.2223-4292.2015.03.07